Numerical simulations of p-wave fermions in a one-dimensional harmonic trap

Marc Camus Sais

Supervisors: Bruno Juliá Díaz, Abel Rojo Francàs

Departament de Física Quàntica i Astrofísica, Facultat de Física, Universitat de Barcelona

July 7, 2025

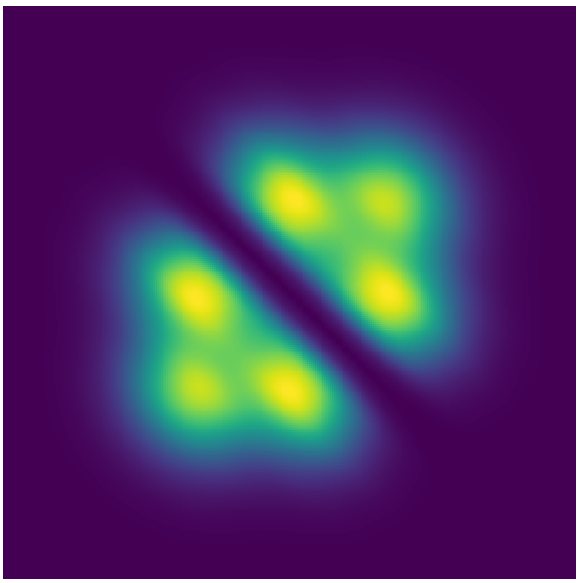

Master in Quantum Science and Technology Barcelona

UNIVERSITAT DE BARCELONA

Numerical simulations of p-wave fermions in a one-dimensional harmonic trap

Marc Camus Sais

Supervised by: Bruno Juliá Díaz, Abel Rojo Francàs

Departament de Física Quàntica i Astrofísica, Facultat de Física, Universitat de Barcelona, E-08028 Barcelona, Spain

7 July 2025

We consider a system of N spin-aligned p-wave fermions confined within a one-dimensional harmonic trap. We study the energy spectrum and ground state properties across different regimes of interaction strength by performing numerical calculations. We compute the particle density and the eigenvalues of the one-body density matrix. Additionally, we study two-particle properties by calculating the pair correlation matrix. In the infinitely interacting limit, our results coincide with those of a fermionic Tonks-Girardeau gas. We analyze the discontinuity behavior near the non-interacting limit and provide an explanation. We propose a novel square well representation of the p-wave interaction in discrete space. We demonstrate the efficiency of this representation by comparing the results obtained with it to those obtained from analytical solutions and other numerical methods. We simulate the dynamics of the system after altering a parameter of the system, such as the trap depth or the interaction strength. We compute spectral properties of the system by analyzing the Fourier transform of the time-dependent spatial spread of the wave function.

Keywords: p-wave, square well, spectrum, density of particles, occupation numbers, pair correlation, breathing, quench

Acknowledgments

I would like to express my gratitude to my supervisors, Bruno Juliá Díaz and Abel Rojo Francàs, for their invaluable guidance throughout the course of this project. They have made it an unforgettable experience. Additionally, I also wish to extend my sincere appreciation to Grigori Astrakharchik and Joan Martorell for the insightful discussions we have shared during this work. I thank the entire ManboQu (Many Body Quantum) team, with particular acknowledgment to Guillem Lancis, Marta Domínguez, Héctor Briongos, and Eric Sánchez, for their valuable contributions. Last but not least, I would like to thank my family and friends for always supporting me.

Marc Camus Sais: marc.camus.sais@gmail.com

Contents

1 Introduction

The use of ultracold gases as an experimental platform enables precise control over interactions between atoms, as well as fine-tuning of system parameters such as geometry, dimensionality, and particle number [1, 2]. This high degree of control makes them an ideal testbed for simulating complex quantum many-body systems and realizing exotic phases of matter [3, 4]. Significant advancements in trapping and cooling techniques [5, 6] have enabled the confinement of cold atomic gases in a one-dimensional ($1D$) regime. This has been achieved using waveguides with tight transverse confinement [7, 8]. The quasi-$1D$ regime is achieved when the chemical potential, μ, and the thermal energy, $k_B T$, are smaller than the level spacing of the transverse oscillator, $\hbar\omega_\perp$ [9]. Under these conditions, the longitudinal motion prevails over other directions, and the system can effectively be considered as $1D$.

In this thesis, we study a $1D$ system comprising N spin-aligned fermions with a p-wave contact interaction, confined in a harmonic potential. This problem is solved analytically for two particles and any value of the interaction strength [10]. For a general number of particles, analytical solutions are only known in two limits: the non-interacting limit and the infinitely interacting limit. In the infinitely interacting limit, the system is solvable by mapping the original Hamiltonian to that of an ideal Bose gas [11]. The ground state energy of infinitely interacting p-wave fermions is equal to the ground state energy of non-interacting bosons. This mapping is analogous to that between an impenetrable Bose gas and ideal fermions [12, 13]. In this case, the ground state energy of non-interacting fermions is equal to that of infinitely repulsive bosons. Outside these limits, the p-wave problem has to be solved numerically. However, this problem cannot be addressed using standard numerical approaches. The p-wave interaction can be represented as a boundary condition on the wave function [14, 15, 16], specifically at the intersection point of two fermions $x_i = x_j^{\pm}$, where $x_j^{\pm} = x_j \pm \epsilon$ with $\epsilon \ll 1$. This property, combined with the anti-symmetric wave functions arising from the fermionic nature of the particles, gives rise to discontinuous wave functions when two fermions are at the same position, $x_i = x_j$. These discontinuities complicate most numerical methods.

The structure of this thesis is as follows. In Sec. 2, we present the Hamiltonian of the system, along with the three cases for which the solution has been found analytically. The present study also investigates the relationship between the p-wave boundary condition and the interaction strength by examining the case of two fermions. In Sec. 3, we present the two numerical methods employed to solve this system. The first method involves transforming our fermionic p-wave system into a bosonic s-wave system, which is solved using standard numerical approaches. The second approach involves using a novel representation of the p-wave interaction as a square well in discrete space. This representation yields results consistent with those obtained by mapping the fermionic problem into the bosonic. In Sec. 4, we examine the ground state properties of our system. First, we compare the spectrum obtained via the mapping with the spectrum obtained using the discrete square well representation. Second, we focus on two main properties of the one-body density matrix: the density of particles and the eigenvalues of the one-body density matrix. Finally, we study two-particle properties by computing the pair correlation matrix. In Sec. 5, we examine the subsequent behavior of the system following an abrupt modification of its parameters. Spectral properties are obtained by analyzing the Fourier frequencies of the time-dependent spatial spread of the wave function, $\sum_i \langle x_i^2 \rangle$. Finally, in Sec. 6, we

summarize and present the main conclusions of our work.

2 Hamiltonian of the system

We consider a system of N spin-aligned fermions in a $1D$ harmonic trap. In this situation, the spin wave function is magnetically frozen in the configuration $\uparrow_1\uparrow_2 \ldots \uparrow_N$. Therefore, the spatial wave function must be antisymmetric to fulfill the fermionic statistics. At low energies, the dominant interaction is the s-wave scattering [17]; however, due to the antisymmetric spatial wave function, this interaction is forbidden. Consequently, the predominant interaction observed is the p-wave interaction. The Hamiltonian of the system is [18]

$$\hat{\mathcal{H}}_{\mathrm{F}} = \sum_{i=1}^{N}\left(-\frac{\hbar^2}{2m}\partial_{x_i}^2 + \frac{1}{2}m\omega^2 x_i^2 - \sum_{j>i}^{N} g_{\mathrm{F}}\delta'(x_i - x_j)\hat{\partial}_{ij}\right), \tag{1}$$

where $\delta'(x_i - x_j) \equiv \partial_{x_{ij}}[\delta(x_i - x_j)]$ being $x_{ij} \equiv x_i - x_j$, and $\hat{\partial}_{ij}$ is the regularized operator

$$\hat{\partial}_{ij}\psi = \frac{1}{2}\left(\partial_{x_i}\psi|_{x_i=x_j^+} - \partial_{x_j}\psi|_{x_i=x_j^-}\right). \tag{2}$$

The $1D$ scattering length, a_{F}, is defined as the ratio

$$\psi|_{x_i=x_j^+} = -\psi|_{x_i=x_j^-} = -\frac{a_{\mathrm{F}}}{2}\left(\partial_{x_i} - \partial_{x_j}\right)\psi|_{x_i=x_j^\pm}, \tag{3}$$

and is related to the interaction strength as $g_{\mathrm{F}} = 2a_{\mathrm{F}}\hbar^2/m$. Consequently, modifying the interaction strength changes the ratio between the wave function and its derivative at $x_i = x_j^\pm$. Therefore, the p-wave interaction imposes a boundary condition at $x_i = x_j^\pm$. The combination of antisymmetry under the exchange of two fermions and this boundary condition results in a discontinuous wave function when two fermions occupy the same position [18, 10].

In general, the spectrum of this Hamiltonian has not been found analytically. However, analytical solutions have been found in three cases: in the non-interacting limit ($g_{\mathrm{F}} \to 0^-$), the fermionic Tonks-Girardeau limit ($g_{\mathrm{F}} \to \pm\infty$) [11], and for two fermions with arbitrary interaction strength [10].

2.1 Two analytically solvable limits

There are analytical solutions for two different limits of spin-aligned p-wave fermions in a harmonic trap, valid for any number of particles. In the absence of interactions, the system is the Fermi gas. The solutions to the Schrödinger equation are the single-particle eigenstates of the harmonic oscillator. The fermionic nature of the particles involves indistinguishability and the Pauli exclusion principle. Therefore, the ground state wave function is given by a Slater determinant of the N lowest energy states of the harmonic oscillator

$$\Psi_{\mathrm{F}}(x_1, \ldots, x_N) = \frac{1}{\sqrt{N!}}\begin{vmatrix} \phi_0(x_1) & \phi_1(x_1) & \cdots & \phi_N(x_1) \\ \phi_0(x_2) & \phi_1(x_2) & \cdots & \phi_N(x_2) \\ \vdots & \vdots & \ddots & \vdots \\ \phi_0(x_N) & \phi_1(x_N) & \cdots & \phi_N(x_N) \end{vmatrix}, \tag{4}$$

with energy $E_{\mathrm{F}} = \hbar\omega N^2/2$.

In the infinitely interacting limit, the system is known as the fermionic Tonks-Girardeau (FTG) gas [11]. In this regime, the system maps to an ideal Bose gas. The ground state wave function is given by

$$\Psi_{\mathrm{F}}(x_1,\ldots,x_N) = \mathcal{A}(x_1,\ldots,x_N)\Psi_{\mathrm{B}}(x_1,\ldots,x_N), \tag{5}$$

where $\Psi_{\mathrm{B}}(x_1,\ldots,x_N) = \prod_{i=1}^{N}\phi_0(x_i)$ is the wave function of the ideal Bose gas, $\phi_0(x)$ denoting the ground state of a single particle in the harmonic trap. $\mathcal{A}$ is the unit antisymmetric function

$$\mathcal{A}(x_1,\ldots,x_N) = \prod_{1\le i<j\le N}\mathrm{sgn}(x_i - x_j). \tag{6}$$

The ground state energy is $E_{\mathrm{F}} = N\hbar\omega/2$. Recently, a novel expression for the ground state wave function of the FTG gas has been proposed in second quantization [19]. It is based on the occupation numbers and paired natural orbitals of the one-body density matrix.

2.2 Two p-wave fermions in a harmonic trap

We now turn our attention to a system of two spin-aligned p-wave fermions trapped in a harmonic potential. This problem has been solved analytically [10]. The Hamiltonian of this system can be expressed in terms of the center of mass (CM) coordinate, $X = (x_1 + x_2)/2$, and the relative position between the two particles, $x = x_1 - x_2$,

$$\hat{\mathcal{H}}_{\mathrm{F}} = -\frac{\hbar^2}{2M}\frac{d^2}{dX^2} + \frac{1}{2}M\omega^2X^2 - \frac{\hbar^2}{2\mu}\frac{d^2}{dx^2} + \frac{1}{2}\mu\omega^2x^2 - g_{\mathrm{F}}\delta'(x)\hat{\partial}_x, \tag{7}$$

where $M = 2m$ is the CM mass, and $\mu = m/2$ is the reduced mass. This Hamiltonian is separable and, consequently, the wave function can be written as $\Psi_{\mathrm{F}}(x_1,x_2) = \psi_{\mathrm{CM}}(X)\psi_{\mathrm{rel}}(x)$ with energy $E_{\mathrm{F}} = E_{\mathrm{CM}} + E_{\mathrm{rel}}$. The solutions of the Schrödinger equation for the CM are the harmonic oscillator wave functions with energy $E_{\mathrm{CM}} = (n + 1/2)\hbar\omega$. The relative energies are given by

$$\frac{g_{\mathrm{F}}}{a_\mu^3} = \hbar\omega\frac{\Gamma\left(-\frac{E_{\mathrm{rel}}}{2\hbar\omega} + \frac{1}{4}\right)}{2\Gamma\left(-\frac{E_{\mathrm{rel}}}{2\hbar\omega} + \frac{3}{4}\right)}, \tag{8}$$

where $a_\mu = \sqrt{\hbar/(\mu\omega)}$ is the harmonic oscillator length. The relative wave function is

$$\psi_{\mathrm{rel}}(x) \propto \frac{\Gamma(-\nu)}{\sqrt{a_\mu}}\frac{x}{a_\mu}\exp\left(-\frac{x^2}{2a_\mu^2}\right)U\left(-\nu,\frac{3}{2},\frac{x^2}{a_\mu^2}\right), \tag{9}$$

where ν is related to the energy as $E_{\mathrm{rel}} = (2\nu + 3/2)\,\hbar\omega$. The ground state relative wave function depends on the boundary condition in Eq. (3), imposed by the p-wave interaction. Fig. 1a displays the relative energy of the low-lying spectrum as a function of the interaction strength. In the infinitely interacting limit, the ground state energy converges to $E_{\mathrm{rel}} = \hbar\omega/2$, as expected for the FTG case. The energy increases monotonically as the interaction strength increases from $-\infty$ to 0. At $g_{\mathrm{F}} = 0$, a discontinuity appears in the ground state energy. For $g_{\mathrm{F}} \to 0^-$, the energy approaches to the non-interacting limit $E_{\mathrm{rel}} = 3\hbar\omega/2$, while for $g_{\mathrm{F}} \to 0^+$, the energy diverges to $E_{\mathrm{rel}} \to -\infty$. For positive interaction strengths, the energy increases with the interaction strength and converges again to the FTG limit in the infinitely interacting case.

Fig. 1b illustrates the ground state relative wave function, $\psi_{\mathrm{rel},0}(x)$, for different interaction strengths. In the infinitely interacting limit, $\psi'_{\mathrm{rel},0}(0^{\pm}) = 0$ while $\psi_{\mathrm{rel},0}(0^{\pm})$ remains

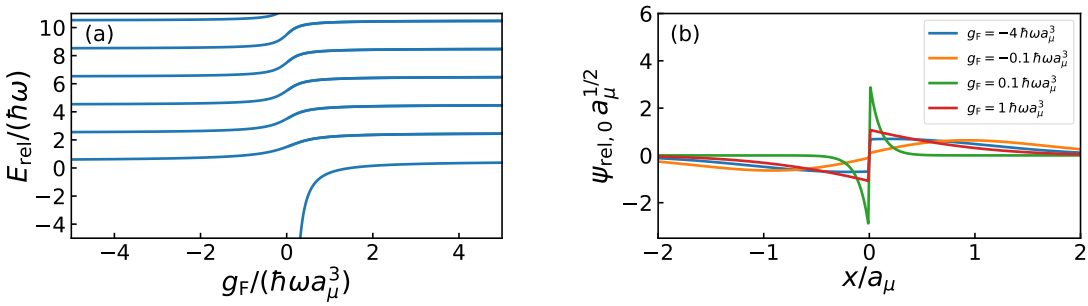

Figure 1: System of two p-wave fermions in a harmonic trap. Panel (a) shows the relative energy low-lying spectrum as a function of the interaction strength. Panel (b) shows the relative wave function for different interaction strengths. The blue, orange, green and red lines correspond to $g_{\mathrm{F}} = -4\,\hbar\omega a_\mu^3$, $g_{\mathrm{F}} = -0.1\,\hbar\omega a_\mu^3$, $g_{\mathrm{F}} = 0.1\,\hbar\omega a_\mu^3$, $g_{\mathrm{F}} = 1\,\hbar\omega a_\mu^3$, respectively.

finite, corresponding to the FTG gas. As the interaction strength increases from $-\infty$ to 0, the discontinuity at the origin becomes less pronounced. At $g_{\mathrm{F}} = 0$, a discontinuity emerges in the behavior of the ground state. The p-wave boundary condition forces the system to adopt a different configuration on either side of this point. In the limit $g_{\mathrm{F}} \to 0^-$, the ground state converges to the non-interacting fermionic solution, where the wave function is continuous. This solution has the same sign for both $\psi'_{\mathrm{rel},0}(x = 0^{\pm})$ and $\psi_{\mathrm{rel},0}(0^+)$, allowing the wave function to accommodate in this solution. Nevertheless, when $g_{\mathrm{F}} > 0$, the boundary condition enforces opposite signs for both $\psi'_{\mathrm{rel},0}(0^{\pm})$ and $\psi_{\mathrm{rel},0}(0^+)$, requiring the wave function to adopt a different form. In the limit $g_{\mathrm{F}} \to 0^+$, the relative wave function exhibits an infinite discontinuity at the origin. This indicates that both fermions are located next to each other. For positive interaction strengths, this discontinuity at the origin decreases as the interaction strength increases.

The kinetic energy is related to the curvature of the wave function; as the curvature increases, so does the kinetic energy. The system increases E_{rel} by adding nodes to the relative wave function. However, due to the odd parity of the relative wave function, excitations introduce two additional nodes. Therefore, the n-th excited relative wave function has $2n$ nodes. The ground state has no nodes in its relative wave function; the first excited state has two nodes, the second has four, and this pattern continues successively.

3 Numerical methods

We now consider the general case of several p-wave fermions interacting with arbitrary interaction strength. Two particular features of the interaction complicate the computations. First, finding discontinuous wave functions at $x_i = x_j$ for $i \neq j$, while maintaining antisymmetry under particle exchange, is challenging. Solving the problem with exact diagonalization (ED) requires a basis set that incorporates both the discontinuity and the antisymmetry conditions, which is non-trivial. Second, the interaction is modeled as a distribution, which is only well-defined under integration. This makes it difficult to represent the interaction in terms of the position of the particles. In this section, we present two numerical methods for solving this Hamiltonian.

3.1 Mapping p-wave fermions to s-wave bosons

In this section, we review the previously established mapping [18, 20]. It consists of mapping the problem of p-wave fermions onto s-wave bosons. The bosonic wave function is symmetric under the exchange of particle positions. This symmetry prevents the discontinuities that appear in p-wave fermionic wave functions from occurring in the s-wave bosonic case. Therefore, the wave function of s-wave bosons is numerically easier to handle than that of p-wave fermions.

The spectrum of s-wave bosons with interaction strength g_{B} in a harmonic trap is equivalent to that of p-wave fermions with interaction strength $g_{\mathrm{F}} = -4\hbar^4/(m^2 g_{\mathrm{B}})$ [18]. We now show how to derive this relation. Consider N spin-aligned bosons trapped in a one-dimensional harmonic potential. The Hamiltonian of the system is [10, 18, 21]

$$\hat{\mathcal{H}}_{\mathrm{B}} = \sum_{i=1}^{N} \left(-\frac{\hbar^2}{2m}\partial_{x_i}^2 + \frac{1}{2}m\omega^2 x_i^2 + \sum_{j>i}^{N} g_{\mathrm{B}}\hat{\delta}_{ij} \right), \tag{10}$$

where the operator $\hat{\delta}_{ij}$ is defined by

$$\hat{\delta}_{ij}\psi = \frac{1}{2}\left(\psi|_{x_i=x_j^+} + \psi|_{x_i=x_j^-} \right) \delta(x_i - x_j). \tag{11}$$

The $1D$ scattering length, a_{B}, is defined as the ratio

$$\psi|_{x_i=x_j^+} = \psi|_{x_i=x_j^-} = -\frac{a_{\mathrm{B}}}{2}\left(\partial_{x_i} - \partial_{x_j}\right)\psi|_{x_i=x_j^\pm}, \tag{12}$$

and is related to the interaction strength as $g_{\mathrm{B}} = -2\hbar^2/(m a_{\mathrm{B}})$. Consequently, changing the interaction strength changes the ratio between the wave function and its derivative at $x_i = x_j^\pm$. Thus, the s-wave interaction imposes a boundary condition at $x_i = x_j^\pm$.

Outside the range of interaction (i.e., when $x_i \neq x_j$), the fermionic and bosonic Hamiltonians are identical. Since both the p-wave and s-wave interactions can be represented as boundary conditions at $x_i = x_j^\pm$ [14, 15, 16], the energy spectra are identical when these boundary conditions coincide. This occurs when $a_{\mathrm{F}} = a_{\mathrm{B}}$, yielding the relation $g_{\mathrm{F}} = -4\hbar^4/(m^2 g_{\mathrm{B}})$. This relation is used to map between the fermionic and bosonic systems. Although the spectra of both systems are the same, the symmetries of their wave functions differ. The eigenfunctions are related by

$$\Psi_{\mathrm{F}}(x_1, \ldots, x_N) = \mathcal{A}(x_1, \ldots, x_N)\Psi_{\mathrm{B}}(x_1, \ldots, x_N). \tag{13}$$

We solve the Schrödinger equation using the Hamiltonian from Eq. (10) by applying the optimized ED method (see Appendix A for details).

3.2 Square well representation of the p-wave interaction

The second method is based on a new proposal to represent the p-wave interaction in discrete space. In this framework, the s-wave interaction is well-known to be represented by a square well of depth $g_{\mathrm{B}}/\Delta x$ at mesh points where $x_i = x_j$, with Δx denoting the spacing of the points in the mesh. We extend this idea by proposing a square well that captures the physics of the p-wave interaction.

3.2.1 Derivation

First, we consider a p-wave fermionic system whose eigenstates and spectrum are analytically known. An interaction potential that reproduces the same spectrum and eigenstates as the original problem can be determined by solving the following equation:

$$V_{\text{int}}(x_1,\dots,x_N) = E_{\text{F}} + \frac{\sum_{i=1}^{N} \frac{\hbar^2}{2m}\partial_{x_i}^2 \Psi_{\text{F}}(x_1,\dots,x_N)}{\Psi_{\text{F}}(x_1,\dots,x_N)} - V(x_1,\dots,x_N), \tag{14}$$

where $V(x_1,\dots,x_N)$ is the external potential. To solve this equation, the spectrum and eigenstates of the problem must be known beforehand.

We consider the system of two spin-aligned p-wave fermions in free space, for which the solutions are known. The Hamiltonian of the system is

$$\hat{\mathcal{H}}_{\text{F}} = -\frac{\hbar^2}{2m}\partial_{x_1}^2 - \frac{\hbar^2}{2m}\partial_{x_2}^2 - g_{\text{F}}\delta'(x_1-x_2)\hat{\partial}_{12}. \tag{15}$$

This Hamiltonian is separable in the CM coordinates, X, and the relative position between the two particles, x. The Hamiltonian of the CM has only the kinetic term. Therefore, the solutions to the CM Hamiltonian are plane waves. For $g_{\text{F}} > 0$, the relative Hamiltonian has a bound state with wave function [22]

$$\psi_{\text{rel}}(x) = \sqrt{\frac{\hbar^2}{2\mu g_{\text{F}}}}\text{sgn}(x)e^{-|x|\hbar^2/(\mu g_{\text{F}})}, \tag{16}$$

with energy $E_{\text{rel}} = -\hbar^6/(2\mu^3 g_{\text{F}}^2)$. This wave function and energy are used to solve Eq. (14).

In order to solve the problem numerically in position space, we discretize the space. The mesh of the discrete space determines the shape of the potential. At $x = 0$, the function $\text{sgn}(x)$ is ill-defined. If $\text{sgn}(x=0)$ is assumed to be equal to zero, then $V_{int}(x = 0) = \infty$, which results in an infinite term in the Hamiltonian that prevents numerical diagonalization. Therefore, the mesh must exclude the point $x = 0$. We use the mesh $\{-L, -L+\Delta x, \dots, -\Delta x, \Delta x, \dots, L-\Delta x, L\}$ to find the spectrum. On this mesh, the discrete square well is non-zero at the points $x = \pm\Delta x$ with height

$$\begin{aligned} V_{x=\Delta x} = V_{x=-\Delta x} &= \frac{\hbar^2}{2\mu}\frac{\psi_{rel}(0) - 2\psi_{\text{rel}}(-\Delta x) + \psi_{\text{rel}}(-2\Delta x)}{\Delta x^2 \psi_{\text{rel}}(-\Delta x)} + E \\ &= \frac{\hbar^2}{\mu\Delta x^2}\left(\frac{e^{-\gamma}}{2} - 1 - \frac{\gamma^2}{2}\right), \end{aligned} \tag{17}$$

where $\psi_{\text{rel}}(0) = 0$, and $\gamma \equiv \Delta x\hbar^2/(\mu g_{\text{F}})$. Using the same method, we find the square well representation of the s-wave interaction (see Appendix B). In this case, the depth of the square well is proportional to g_{B}, which provides a straightforward discretization of $\delta(x)$. However, for the p-wave interaction, the depth is not simply proportional to g_{F}, making it impossible to find a representation of the operator $\delta'(x)\hat{\partial}_x$ in the discrete space.

In conclusion, we have introduced a new way to represent the p-wave interaction in discrete spaces. Note that this interaction is non-zero only at the points where $x_i = x_j \pm \Delta x$. If additional points are placed between the points $x_i = x_j \pm \Delta x$, the representation becomes invalid. Therefore, the interaction must be defined such that it is non-zero only at $x_i = x_j \pm \Delta x$, with no intermediate points. A similar limitation arises for the s-wave interaction.

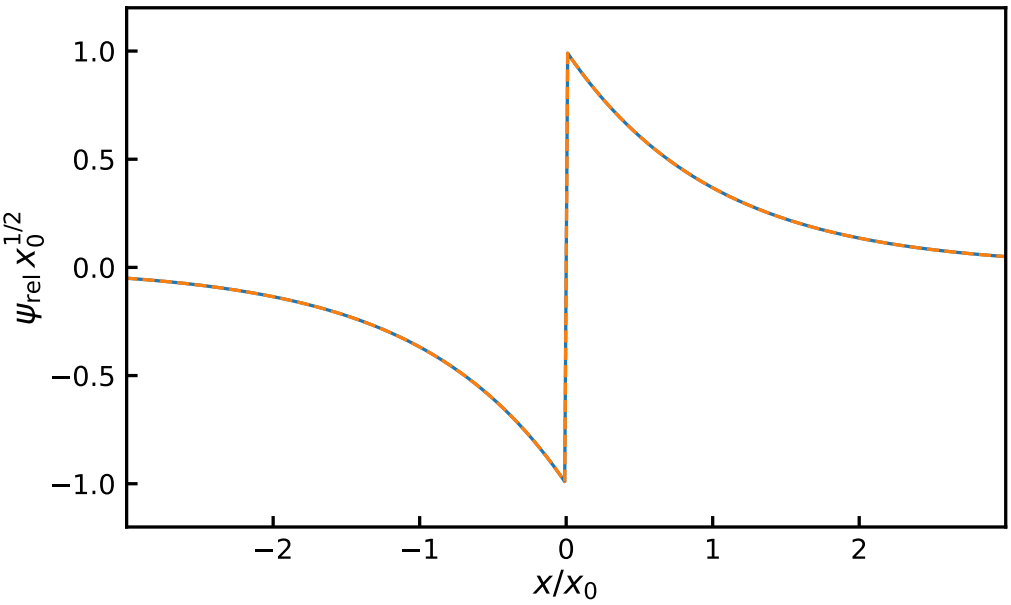

Figure 2: Relative ground state wave function for two free p-wave fermions as a function of the position, x/x_0, where $x_0 = \mu g_{\mathrm{F}}/\hbar^2$. The solid blue line shows the results obtained by diagonalizing the Hamiltonian in discrete space with the potential given by Eq. (17). The orange dashed line shows the analytical results from Eq. (16).

3.2.2 Testing the potential

In this section, we benchmark the performance of the potential defined in Eq. (17) by comparing numerical results with the corresponding analytical solution. Specifically, we model the p-wave interaction using the square well and compute the spectrum by diagonalizing the Hamiltonian in a discretized spatial basis. We begin by considering the system of two free p-wave fermions. The numerically computed relative ground-state energy is $E_{\mathrm{rel}} = -0.500005\,\hbar^6/(\mu^3 g_{\mathrm{F}}^2)$, which is consistent with the analytical results [22]. In Fig. 2, we compare the numerically obtained wave function of the bound state, ψ_{rel}, with the analytical expression given in Eq. (16). The two results match exactly, confirming that the potential in Eq. (17) accurately reproduces the p-wave boundary condition for free p-wave fermions.

The potential given by Eq. (17) has been derived for two free fermions. We use the same expression to simulate p-wave fermions in a harmonic potential. Fig. 3 shows the relative energy low-lying spectrum, E_{rel}, and the corresponding relative eigenfunctions, $\psi_{\mathrm{rel}}(x)$. The ground and excited state energies are accurately reproduced. Moreover, the numerically computed wave functions for both the ground and excited states closely match the analytical results. We have obtained successful results in two p-wave fermionic problems. Eq. (17) appears to be a general representation of the p-wave interaction as a square well.

We study the convergence of the ground state energy of two p-wave fermions in a harmonic trap as a function of the discretization spacing. As $\Delta x \to 0$, the difference between the analytical and numerical energies should approach zero, $E_{\mathrm{th}} - E_{\mathrm{sim}} \to 0$.

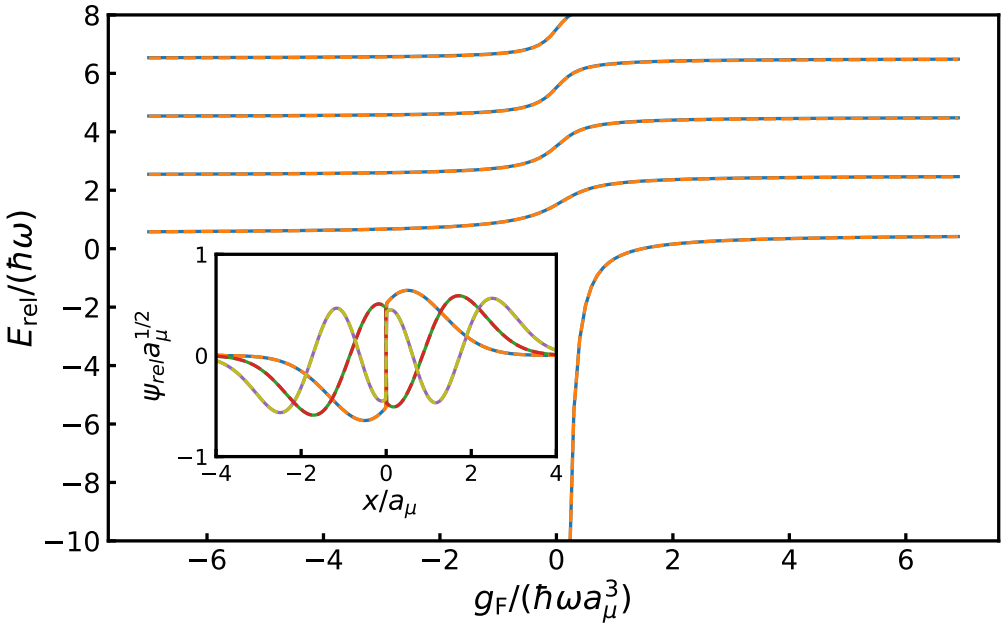

Figure 3: Relative energy spectrum of low-lying states for two p-wave fermions in a harmonic trap as a function of the interaction strength. The solid blue lines show the results obtained by diagonalizing the Hamiltonian in position space with the potential given by Eq. (17). The orange dashed lines represent the analytical results from Eq. (8). The inset displays the relative wave functions for $g_{\mathrm{F}} = -1\,\hbar\omega a_\mu^3$. The solid blue, green and purple lines correspond to the numerically computed wave functions of the ground, first excited and second excited states, respectively. The dashed lines show the corresponding analytical wave functions.

Fig. 4a shows the error, $|E_{\mathrm{th}} - E_{\mathrm{sim}}|$, as a function of the interaction strength for various values of Δx. The error decreases as Δx becomes smaller, for all interaction strengths considered. Fig. 4b presents the convergence of this error with respect to the spacing, demonstrating a linear dependence, $|E_{\mathrm{th}} - E_{\mathrm{sim}}| \propto \Delta x$.

In this work, we perform calculations in discrete space using the square well representation of the p-wave interaction, allowing us to compute energies for systems with larger number of particles. We determine the spectrum of the system using two different numerical methods. The first method involves diagonalizing the Hamiltonian in position space. The second method employs variational Monte Carlo (VMC), which requires a trial wave function with variational parameters.

We design the trial wave function based on the ground state wave function for two p-wave fermions in a harmonic trap

$$\Psi_{\mathrm{F}}(x_1, x_2) \propto \frac{(x_2 - x_1)}{a_m^2} e^{-(x_1^2+x_2^2)/(2a_m^2)} U\left(-\nu, \frac{3}{2}, \frac{(x_2-x_1)^2}{2a_m^2}\right), \tag{18}$$

where $a_m = \sqrt{\hbar/(m\omega)}$ and ν is obtained by solving Eq. (8). In the FTG limit, ν converges to $\nu = -0.5$. In this limit,

$$U\left(-\nu, \frac{3}{2}, \frac{(x_2-x_1)^2}{2a_m^2}\right) \to \frac{\sqrt{2}a_m}{\sqrt{(x_2-x_1)^2}}. \tag{19}$$

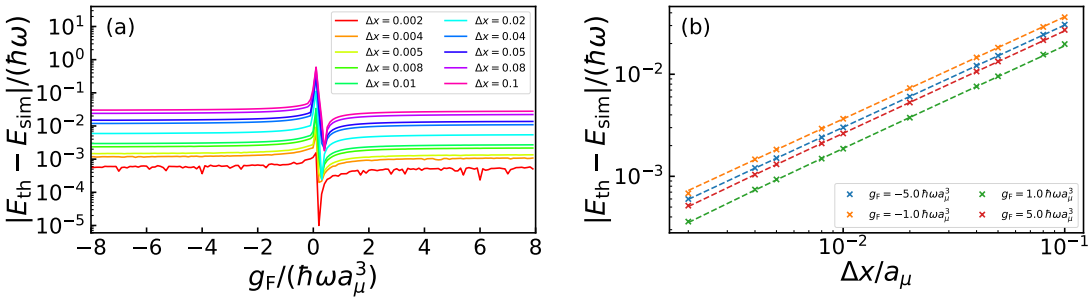

Figure 4: Absolute value of the energy difference between the analytical and the numerical results, $|E_{\text{th}} - E_{\text{sim}}|$, for the relative energy. Panel (a) shows $|E_{\text{th}} - E_{\text{sim}}|$ as a function of the interaction strength for different values of Δx. The y-axis is on a log scale. The values of Δx in the legend are given in units of the harmonic oscillator. Panel (b) shows $|E_{\text{th}} - E_{\text{sim}}|$ as a function of Δx for various interaction strengths. Both axes are logarithmic. The dashed lines show the linear fit of $|E_{\text{th}} - E_{\text{sim}}|$ as a function of Δx for different interaction strengths, indicating a proportional dependence.

Therefore, in the FTG limit, the $\text{sgn}(x_i - x_j)$ factor in the wave function arises from a combination of $U(-\nu, 3/2, (x_i - x_j)^2/(2a_m^2))$ and $(x_i - x_j)/a_m$. A possible trial function for N p-wave fermions in a harmonic trap is [23]

$$\Psi_{\text{F}}(x_1, \ldots, x_N) = \frac{\mathcal{N}}{a_m^{N/2}} \prod_{i=1}^{N} e^{-x_i^2/(2a_m^2)} \prod_{1 \le j < k \le N} \frac{x_k - x_k}{a_m} U\left(-\nu_\alpha, \frac{3}{2}, \frac{\alpha^2 (x_j - x_k)^2}{2a_m^2}\right), \quad (20)$$

where $\mathcal{N}$ is a normalization constant and α is the variational parameter. The value of ν_α is obtained by solving the equation

$$\sqrt{2}\hbar\omega a_m^3 \Gamma\left(-\nu_\alpha - \frac{1}{2}\right) = g_{\text{F}} \alpha \Gamma\left(-\nu_\alpha\right). \quad (21)$$

However, this approach is computationally demanding. To overcome this difficulty, we use an adapted trial function from [23]:

$$\Psi_\alpha(x_1, \ldots, x_N) = \frac{\mathcal{N}}{a_m^{N/2}} \exp\left(-\sum_{i=1}^{N} \frac{x_i^2}{a_m^2}\right) \prod_{1 \le j < k \le N} \phi_\alpha\left(\frac{x_j - x_k}{a_m}\right), \quad (22)$$

where $\mathcal{N}$ is the normalization constant and

$$\phi_\alpha(x) = \text{sgn}(x)\left(1 - \frac{e^{-\alpha|x|}}{1 - \frac{\alpha g_{\text{F}}}{2\hbar\omega a_m^3}}\right), \quad (23)$$

and α is the variational parameter.

4 Ground state properties

The study of ground state (GS) properties provides insight into how the system behaves at its lowest energy. We analyze the energy spectrum for $N = 2$ and $N = 3$ to evaluate the performance of the square well representation of the p-wave interaction. Additionally, we investigate one-particle properties by computing the particle density and the one-body density matrix eigenvalues. Finally, we study two-particle properties by examining the pair correlation matrix.

4.1 Energy spectrum

We compute the energy spectrum using three different methods. The first method involves performing optimized ED on a system of s-wave bosons and mapping the results to p-wave fermions. This approach provides an upper bound on the energy of the system. The second and third methods use the potential deduced in Sec. 3.2. These two methods do not provide an upper bound because they numerically solve a problem with a square well potential that approximates the p-wave interaction. Therefore, both share a common source of error due to the difference between the actual p-wave interaction and the square well representation. The second method involves diagonalizing the Hamiltonian in position space, introducing an additional source of error from computing the energy in discrete space. The third method uses VMC and has two additional sources of error: one from computing the energy variationally and another from statistical uncertainty in the calculations.

Fig. 5 compares the energy spectrum obtained using the three numerical methods as a function of the interaction strength. In general, the energies predicted by the three methods are more similar for negative interaction strengths than for positive ones. However, for higher excited states, the numerical results differ more significantly between methods. Furthermore, for $N = 3$, the VMC results differ from those of the other two methods, which are more consistent with each other. This discrepancy arises because the trial wave function in Eq. (22) does not precisely capture the GS energy, combined with the fact that the energy is more sensitive to the choice of the variational parameter, α. A more accurate selection of the value of the variational parameter yields improved results, particularly for positive interaction strengths.

Fig 5a illustrates the spectrum of two p-wave fermions in a harmonic trap. Unlike the previous figures, Fig 5a displays the total energy, including the CM energy. Focusing on negative interaction strengths, the first curve corresponds to the GS of both the relative and the CM modes. The second curve is similar to the first, but includes a CM excitation. The third and fourth states exhibit similar energies; however, the former corresponds to the first excited state of the relative mode with the CM situated in the GS, while the latter corresponds to the GS of the relative mode with the CM in its third excited state. For positive interaction strengths, the relative GS energy diverges to $-\infty$ as $g_{\mathrm{F}} \to 0^{+}$. Therefore, the first, second, third, and fifth curves correspond to the ground, first, second, and third excited states of the CM, respectively, with the relative mode in its ground state. The fourth curve corresponds to the first excited state of the relative mode with the CM in the GS.

For three fermions, the wave function separates into a CM part and an intrinsic part. Figure 5b shows the total energy for three fermions. For negative interaction strengths, the first, second, and fourth curves correspond to the intrinsic part being in its GS, with the CM in the ground, first excited, and second excited states, respectively. The third curve corresponds to the first intrinsic excited state with the CM in its GS. For positive interaction strengths, the first, second, and third curves correspond to the intrinsic mode in its GS, with the CM in the ground, first excited, and second excited states, respectively. The fourth curve corresponds to the first intrinsic excited state and the CM in its GS.

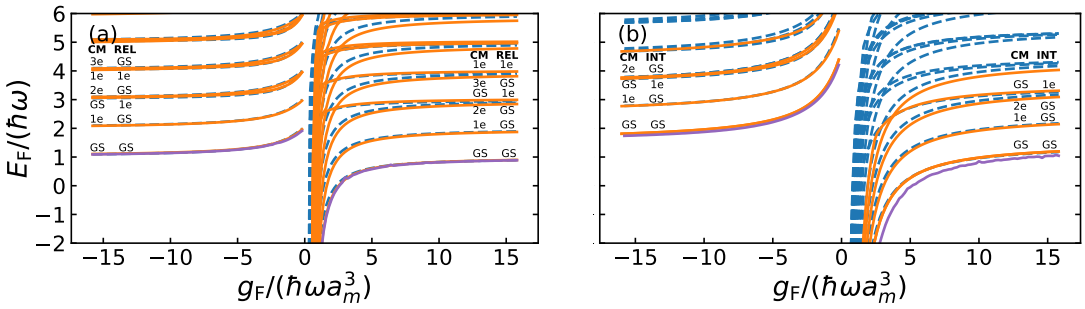

Figure 5: Energy spectrum of N p-wave fermions in a harmonic trap as a function of the interaction strength. The blue dashed lines represent the numerical results obtained using optimized ED on the bosonic Hamiltonian. The orange solid lines show the results from diagonalizing the Hamiltonian in position space with the p-wave interaction modeled as a square well. The purple solid line corresponds to the VMC results, which also use the square well representation of the p-wave interaction. The statistical uncertainty of the VMC is small enough to be negligible in the figure. Panels (a) and (b) correspond to $N = 2$ and $N = 3$, respectively.

4.2 One-body properties

The one-body density matrix (OBDM) is defined as

$$\rho^{(1)}(x, x') = N \int dx_2 \dots dx_N \Psi^*(x', x_2, \dots, x_N)\Psi(x, x_2, \dots, x_N), \tag{24}$$

and is normalized to the number of particles, N. The diagonal of this matrix gives the particle density at position x, $\rho(x) \equiv \rho^{(1)}(x, x)$.

Note that the density profile is the same for fermions with an interaction strength of g_F and for bosons with an interaction strength of $g_B = -4\hbar^4/(m^2 g_F)$. Therefore, we compute the density of particles by performing optimized ED on the system of s-wave bosons. We express the GS wave function in position space and use Eq. (24). We use the bosonic wave function instead of the fermionic one because the $\mathrm{sgn}(x_i - x_j)$ factor in the latter introduces numerical errors in the integrals.

Fig. 6 shows the density profiles of $N = 2$ and $N = 3$ p-wave fermions in a harmonic trap. In the FTG limit, the particle density corresponds to a system of N ideal bosons in the GS

$$\rho(x) = N|\phi_0(x)|^2, \tag{25}$$

where $\phi_0(x)$ is the single-particle GS of the harmonic trap. As the interaction strength increases from $-\infty$ to 0, the density profile flattens and converges to that of a non-interacting system as $g_F \to 0^-$. In the non-interacting limit, the density profile takes the form

$$\rho(x) = |\phi_0(x)|^2 + |\phi_1(x)|^2 + \dots + |\phi_{N-1}|^2, \tag{26}$$

where $\phi_i(x)$ is the i-th single-particle excited state of the harmonic trap. The behavior at $g_F = 0$ is discontinuous. For $g_F \to 0^+$, a peak appears at $x = 0$ that decreases as the interaction strength increases. This peak converges to the FTG gas profile for the limit $g_F \to +\infty$.

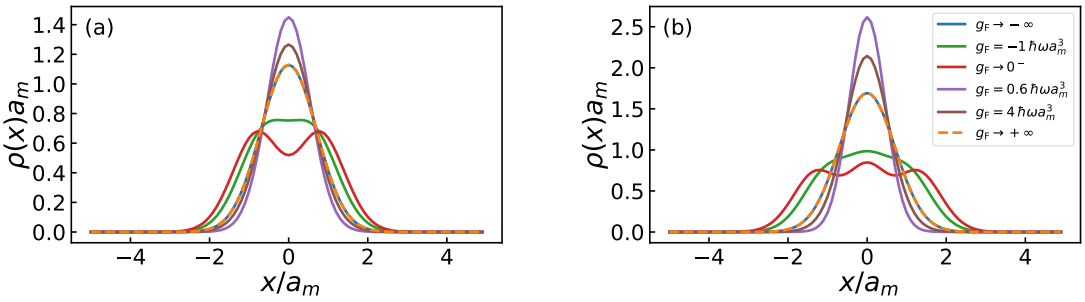

Figure 6: Density profile of the GS for a system of p-wave fermions trapped in a harmonic potential for different interaction strengths. In the limits $g_F \to \pm\infty$, both curves converge to the same profile. Panel (a) corresponds to the case of two fermions, and panel (b) to the case of three fermions.

Despite their different natures, the density of particles in bosonic and fermionic systems is the same. However, computing other quantities reveals characteristic features that distinguish the two systems. The off-diagonal terms of the OBDM differ due to the $\mathrm{sgn}(x_i - x_j)$ factor present in the fermionic wave function. As a result, the eigenvalues, λ, of the OBDM differ between fermions interacting with g_F and bosons interacting with $g_B = -4\hbar^4/(m^2 g_F)$. These differences in the OBDM may lead to distinct physical phenomena in the two systems.

We compute the OBDM by performing optimized ED on the system of s-wave bosons. Next, we express the GS wave function in position space and map it to the fermionic wave function using Eq. (13). We then use Eq. (24) to compute the OBDM and obtain its eigenvalues by diagonalizing it in position space. Fig. 7a shows the dependence of the eigenvalues of the OBDM for the GS in the case of two fermions. Note that all the eigenvalues are doubly degenerate. In the FTG limit, the eigenvalues have an analytical expression [24]

$$\lambda_k^{(2)} = \frac{8}{(\pi(2k-1))^2}, \tag{27}$$

where $k = 1, 2, ...$ As the interaction strength ranges from negative infinity to zero, the two largest eigenvalues increase and converge to one, while the remaining eigenvalues approach zero, as expected in the non-interacting limit. A discontinuity appears in the behavior of the eigenvalues at $g_F = 0$. In the limit $g_F \to 0^+$, the two largest eigenvalues decrease, reaching their minimum values, while the others reach their maxima. In this limit, the particles are strongly correlated, as the relative wave function diverges at $x_1 = x_2^{\pm}$. Therefore, knowing the position of one particle guarantees knowing the position of the other. In the limit $g_F \to +\infty$, the eigenvalues again converge to the FTG limit.

Fig. 7b shows the dependence of the OBDM eigenvalues of the GS for $N = 3$. All the eigenvalues are doubly degenerate, except for the largest one, which is non-degenerate. In the FTG limit, the largest eigenvalue is $\lambda_0^{(3)} = 1$, and the doubly degenerate eigenvalues are

$$\lambda_k^{(3)} = \frac{24}{(2\pi k)^2}. \tag{28}$$

As the interaction strength varies from negative infinity to zero, the largest eigenvalue first decreases slightly and then increases, converging to 1. The second and third eigenvalues

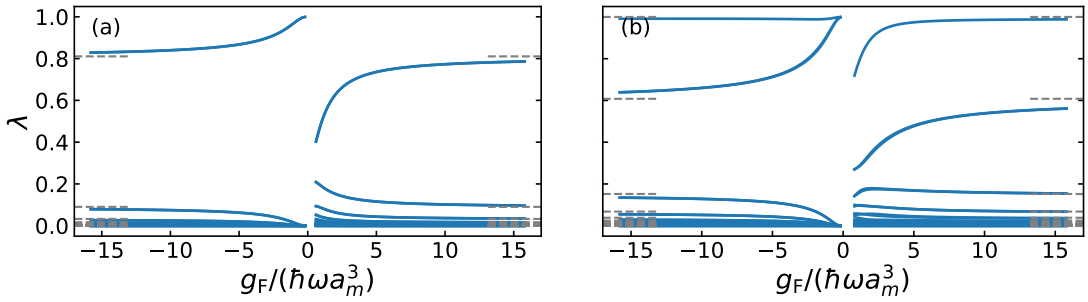

Figure 7: Eigenvalues of the OBDM of the GS for a system of N p-wave fermions in a harmonic trap as a function of the interaction strength. The numerical results are shown as solid blue lines. The analytical values in the FTG limit are shown as dashed gray lines. Panel (a) corresponds to the case of two fermions, where all the eigenvalues are doubly degenerate. Panel (b) shows the case of three fermions, where all the eigenvalues are doubly degenerate except for the largest one, which is non-degenerate.

increase, also converging to 1, while the remaining eigenvalues decrease and converge to zero. At $g_F = 0$, the system behaves analogously to $N = 2$ case, exhibiting a discontinuity in the behavior of the system. In the limit $g_F \to 0^+$, many eigenvalues contribute significantly. As g_F increases, the eigenvalues converge to the FTG limit again.

4.3 Pair correlation

The pair correlation is defined as

$$\rho^{(2)}(x, x') = \frac{N(N-1)}{2} \int dx_3 \dots dx_N |\Psi(x, x', x_3, \dots, x_N)|^2, \tag{29}$$

and is normalized to the number of pairs. This matrix illustrates the degree of correlation between particles. Note that the off-diagonal terms of the pair correlation matrix are identical for fermions with an interaction strength g_F and for bosons with an interaction strength $g_B = -4\hbar^4/(m^2 g_F)$. However, the diagonal terms differ. For p-wave fermions, the diagonal is filled with zeros due to the Pauli exclusion principle. Therefore, we compute the pair correlation matrix using the bosonic wave function in position space via Eq. (29), and manually set the diagonal to zero.

Fig. 8 shows the pair correlation matrix of the GS for three fermions at different interaction strengths (see Appendix C for the pair correlation matrix of the GS for $N = 2$). In the FTG limit, the pair correlation matrix correspond to that of N ideal bosons in the GS, with zero on the diagonal:

$$\rho^{(2)}(x, x') = \frac{N(N-1)}{2} \left[\mathrm{sgn}(x - x')\right]^2 |\phi_0(x)\phi_0(x')|^2, \tag{30}$$

where $[\mathrm{sgn}(x \neq 0)]^2 = 1$ and $[\mathrm{sgn}(0)]^2 = 0$. As the interaction strength increases from negative infinity to zero, fermions separate, approaching the non-interacting limit at $g_F \to 0^-$. In the limit $g_F \to 0^+$, the pair correlation is mostly non-zero near the diagonal and zero elsewhere, indicating a high degree of proximity between fermions. This behavior arises from the divergence of the wave function at $x_i = x_j^{\pm}$. In this limit, particles exhibit a high degree of correlation. Additionally, a maximum appears at the center of the harmonic trap. As the interaction strength increases, the fermions separate again and converge to the FTG limit as $g_F \to +\infty$.

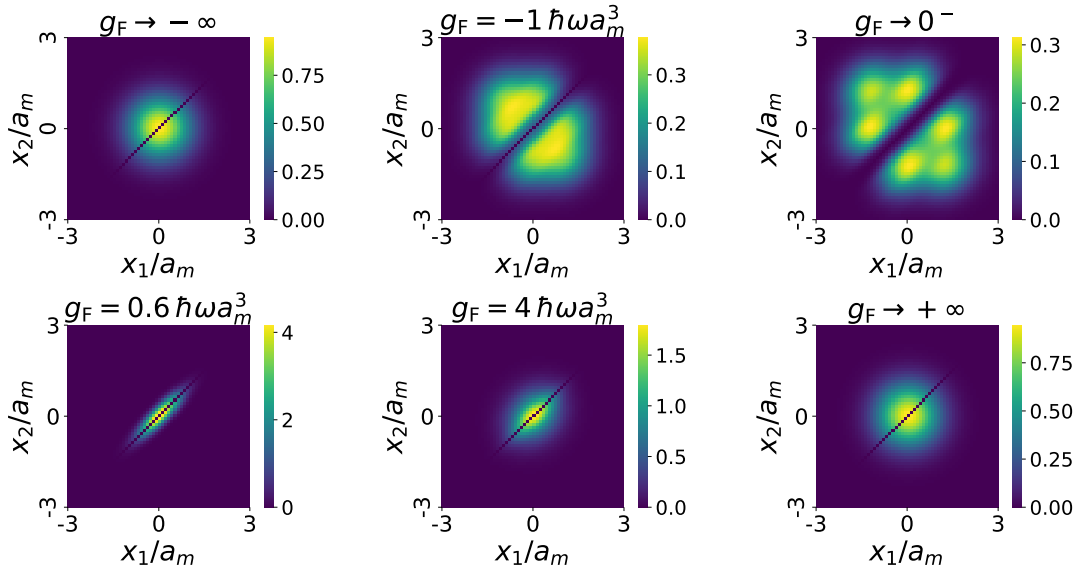

Figure 8: Pair correlation matrix of the GS for three p-wave fermions in a harmonic trap at six different interaction strength values. The limits $g_F \to \pm\infty$ correspond to the FTG limit, while $g_F \to 0^-$ corresponds to the non-interacting limit. The case of $g_F = 0.6\,\hbar\omega a_m^3$ represents a regime where the particles are strongly correlated. The remaining two values correspond to intermediate interaction strengths, illustrating the transition between the limiting cases.

5 Dynamical excitations

Heretofore, the emphasis has been on the static properties of the system. In this section, we examine the dynamics of the system under two distinct sudden perturbations. This reveals the spectral properties of the system.

The oscillation frequencies of the time-dependent spread of the wave function, $\langle\sum_{i=1}^{N} x_i^2\rangle(t)$, are associated with the energy gaps of the spectrum after the perturbation:

$$\begin{aligned}\left\langle\sum_{i=1}^{N} x_i^2\right\rangle(t) = &\sum_{i=1}^{N}\sum_{m} |\langle\phi_m^f|\Psi(0)\rangle|^2\langle\phi_m^f|x_i^2|\phi_m^f\rangle \\ &+\sum_{i=1}^{N}\sum_{1\le n<m\le N} 2\cos(\omega_{mn}t)\,\langle\phi_n^f|\Psi(0)\rangle\langle\phi_m^f|\Psi(0)\rangle\langle\phi_m^f|x_i^2|\phi_n^f\rangle,\end{aligned} \tag{31}$$

where ϕ_m^f represents the m-th excited state of the final Hamiltonian, $\hat{\mathcal{H}}_{\mathrm{F}}^f$, $\Psi(0)$ is the initial state, and $\omega_{mn} \equiv |E_m^f - E_n^f|/\hbar$ being $\hat{\mathcal{H}}_{\mathrm{F}}^f\left|\phi_m^f\right\rangle = E_m^f\left|\phi_m^f\right\rangle$. It is assumed that $\phi_m^f(x_1,\ldots,x_N) \in \mathbb{R}$. While the first term remains constant, the second term exhibits temporal oscillations. These oscillation frequencies are associated with the energy gaps of the final Hamiltonian.

It is also noteworthy that the expectation value of the wave function spread can be written as

$$\left\langle\sum_{i=1}^{N} x_i^2\right\rangle = \left\langle NX^2 + \sum_{1\le j<i\le N}\frac{x_{ij}^2}{N}\right\rangle, \tag{32}$$

where $X = \sum_{i=1}^{N} x_i/N$ denotes the position of the CM, and $x_{ij} = x_i - x_j$ represents the

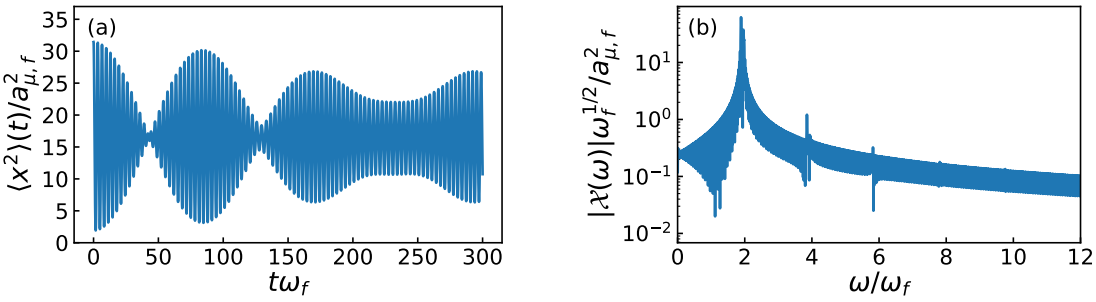

Figure 9: Panel (a) shows the expectation value of the square of the relative position between two fermions in a harmonic trap with an interaction strength of $g_{\mathrm{F}} = -1\,\hbar\omega_f a^3_{\mu,f}$. The presence of multiple oscillatory frequencies is visible. Panel (b) displays the absolute value $|\mathcal{X}(\omega)|$ as a function of ω. Four distinct peaks are observed at $\omega/\omega_f = 1.89, 3.85, 5.82, 7.81$is indeed feasible. The y-axis is shown on a logarithmic scale.

relative position between particles i and j. This decomposition enables the separation of CM excitations from relative modes excitations.

5.1 Breathing

A well-known method for studying the internal structure of a quantum many-body system trapped in a harmonic oscillator is through the excitation of the breathing mode [25, 26]. This is achieve by perturbing the system via changes in the trap of the harmonic oscillator. The system is initially prepared in the GS for a given frequency, ω_0, and interaction strength between fermions, g_{F}. A spontaneous modification in the frequency of the trap, ω_f, is introduced, while the fermionic interaction strength remains unchanged.

This perturbation excites both the CM and the relative modes of the system. It has been established that, due to the change in frequency, $\langle\phi^f_m|\Psi(0)\rangle \neq 0$ if the CM component of ϕ^f_m has the same parity as the CM component of the initial state. The effect of the perturbation on the CM is characterized by the factor $\langle\phi^f_m|X^2|\phi^f_n\rangle$; as a result, the gap of the CM detected by this perturbation is $2\omega_f$. Higher gaps in the CM spectrum are not detected.

We predict the gap of a system of two p-wave fermions by driving their breathing modes. To do so, the initial state is decomposed as $\Psi^0_{\mathrm{F}}(x_1, x_2) = \psi^0_{\mathrm{CM}}(X)\psi^0_{\mathrm{rel}}(x)$, and the excitations of the relative modes are examined. The GS of the initial Hamiltonian $\hat{\mathcal{H}}^0_{\mathrm{F}}$, with trap frequency $\omega_0 = 0.3\,\omega_f$, is used as the starting point for the evolution of the system. The subsequent dynamics are governed by the final Hamiltonian $\hat{\mathcal{H}}^f_{\mathrm{F}}$, with a trap frequency ω_f. Applying the Fourier transform reveals peaks at distinct frequencies

$$\mathcal{X}(\omega) \equiv \mathcal{F}\left[\langle x^2\rangle(t) - \mathbb{E}\left[\langle x^2\rangle(t)\right]\right] = \frac{1}{\sqrt{T}}\int_0^T \left(\langle x^2\rangle(t) - \mathbb{E}\left[\langle x^2\rangle(t)\right]\right) e^{-i\omega t}dt, \qquad (33)$$

where T is the total integration time, $\mathbb{E}\left[\langle x^2\rangle(t)\right] = \int_0^T \langle x^2\rangle(t)dt/T$, and x is the relative position between particles. The term $\mathbb{E}\left[\langle x^2\rangle(t)\right]$ removes the constant component in Eq. (31). Fig. 9a shows $\langle x^2\rangle(t)$ for $g_{\mathrm{F}} = -1\,\hbar\omega_f a^3_{\mu,f}$, where $a_{\mu,f} = \sqrt{\hbar/(\mu\omega_f)}$. The variable under consideration is not centered around zero due to the presence of the constant term.

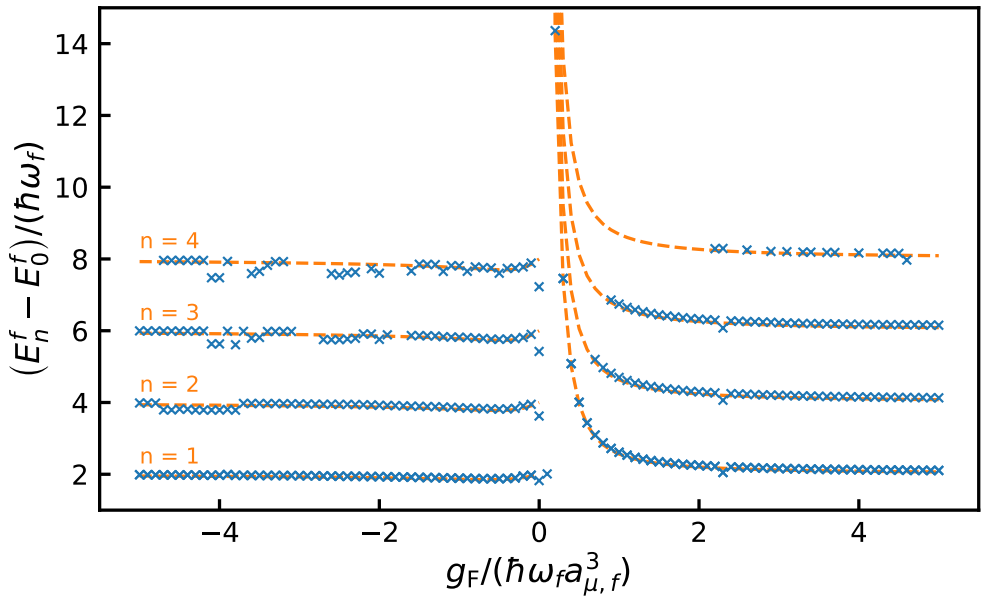

Figure 10: Energy gaps of the final Hamiltonian as a function of the interaction strength. The numerical results, obtained by identifying the peaks in $|\mathcal{X}(\omega)|$, are represented by blue crosses with error bars; however, the error bars are not visible due to the small size. The first, second, third, and fourth dashed orange lines correspond to the energy gaps between the GS and the first, second, third, and fourth excited states, respectively.

Furthermore, the oscillatory behavior exhibited by the system is not solely attributable to a single frequency, but rather to multiple frequencies. This is a consequence of the overlap between the initial state and the eigenstates of the final Hamiltonian. Fig. 9b displays the peaks in the Fourier transform, $\mathcal{X}(\omega)$. It is possible to distinguish four peaks at $\omega/\omega_f = 1.89, 3.85, 5.82, 7.81$. These peaks indicate the energy gaps between the ground state and the excited states of the final Hamiltonian, $\hat{\mathcal{H}}_{\mathrm{F}}^f$.

As illustrated in Fig. 10, a comparison is made between the energy gaps computed from the dynamics of the system and those obtained analytically Eq. (8). This perturbation is capable of exciting all relative modes. The m-th excited state of $\hat{\mathcal{H}}_{\mathrm{F}}^f$ has the form

$$\phi_m^f(x) = \mathcal{N}\frac{x}{a_{\mu,f}^{3/2}}\exp\left(-\frac{x^2}{2a_{\mu,f}^2}\right)U\left(-m,\frac{3}{2},\frac{x^2}{a_{\mu,f}^2}\right), \tag{34}$$

where $\mathcal{N}$ is the normalization constant and $m \in \mathbb{R}$. Therefore,

$$\left\langle \phi_m^f \middle| \frac{x^2}{a_{\mu,f}^2} \middle| \phi_n^f \right\rangle = \left(\frac{3}{2}+2n\right)\left\langle \phi_m^f \middle| \phi_n^f \right\rangle + n\left(\frac{1}{2}+n\right)\left\langle \phi_m^f \middle| \phi_{n-1}^f \right\rangle + \left\langle \phi_m^f \middle| \phi_{n+1}^f \right\rangle, \tag{35}$$

where we use the relation $x^2U(a,b,x^2) = (b-2a)U(a,b,x^2) - a(b-1-a)U(a+1,b,x^2) + U(a-1,b,x^2)$. In the case of general interaction strength, the energy difference between two states is not necessarily $2\hbar\omega_f$. Therefore, Eq. (35) is nonzero, and the perturbation excites all relative modes.

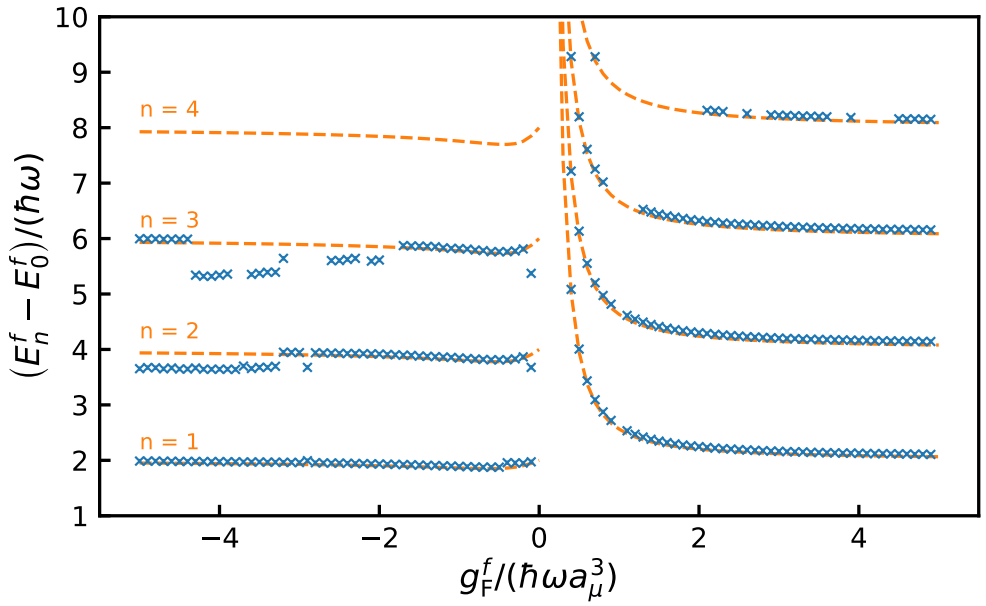

Figure 11: Energy gaps of the final Hamiltonian as a function of the interaction strength. The numerical results are shown as blue crosses with error bars, which are not visible due to their small size. The first, second, third, and fourth dashed orange lines represent the energy gaps between the GS and the first, second, third, and fourth excited states, respectively.

The ability to accurately compute higher energy gaps depends on the value $\left\langle \phi_m^f \right| x^2 \left| \phi_n^f \right\rangle$. In both the non-interacting and infinitely interacting limits, the smallest energy gap is $2\hbar\omega_f$. In the intermediate regime, for negative interaction strengths, the smallest gap is smaller and deviates from $2\hbar\omega_f$, allowing the computation of several gaps. Furthermore, the smallest gaps are computed with greater accuracy. For positive interaction strengths, the smallest gap differs significantly from $2\hbar\omega_f$, enabling a more precise determination of the other gaps.

5.2 Interaction strength quench

The second perturbation involves modifying the interaction strength of the fermions [27, 28]. The system begins in the GS for a Hamiltonian with a given interaction g_F^0, and an abrupt change is applied to the interaction strength, setting it to g_F^f. In this perturbation, only the relative modes of the system are excited. Since the change affects only the interaction term in the Hamiltonian and not the CM, the eigenstates of the CM of the initial Hamiltonian remain eigenstates of the final Hamiltonian. Consequently, $\langle \phi_m^f | \Psi(0) \rangle = 0$ if the initial state, $\Psi(0)$, and ϕ_m^f have different CM components. By analyzing the post-quench dynamics of the system, we can extract the energy gaps between the GS and the excited states.

We predict the energy gaps in a system of two p-wave fermions by performing a quench on the interaction strength. To do this, the initial state is written as $\Psi_F^0(x_1, x_2) = \psi_{CM}^0(X)\psi_{rel}^0(x)$, and we focus on excitations of the relative modes. The system starts in the GS of the initial Hamiltonian $\hat{\mathcal{H}}_F^0$, with interaction strength g_F^0 and then evolves under the final Hamiltonian $\hat{\mathcal{H}}_F^f$ with interaction strength g_F^f. By performing the Fourier trans-

form of $\langle x^2 \rangle(t)$, Eq. (33), we observe peaks at various frequencies. These peaks correspond to the energy gaps between the ground state and excited states of the final Hamiltonian $\hat{\mathcal{H}}_{\mathrm{F}}^{f}$.

As shown in Fig. 11, we compare the energy gaps extracted from observing the dynamics of the system with those obtained analytically. As with the breathing mode excitation, it can be shown that any relative mode can be excited by this quench. The accuracy of the gap calculation is comparable to that achieved using the breathing mode method.

6 Conclusions

In this thesis, we have investigated the properties of N spin-aligned p-wave fermions confined in a one-dimensional harmonic trap. We have developed and applied two numerical strategies to overcome the challenges introduced by the singular nature of the p-wave interaction. The first method exploits a mapping between fermionic and bosonic systems, based on the observation that their spectra are identical. The corresponding eigenstates are related via the fully antisymmetric function $\mathcal{A}(x_1, \ldots, x_N)$. The second method introduces a novel square well representation of the p-wave interaction, which allows direct diagonalization of the Hamiltonian in real space. This formulation also facilitates the use of the VMC method.

We have carried out a comprehensive analysis of the ground-state properties of the system across a broad range of interaction strengths. In the strongly interacting regime, the system approaches the FTG limit, displaying characteristics of an ideal Bose gas. The system exhibits a discontinuity in behavior at $g_{\mathrm{F}} = 0$. As $g_{\mathrm{F}} \to 0^-$, the system behaves like a gas of non-interacting fermions. In contrast, as $g_{\mathrm{F}} \to 0^+$, strong correlations emerge. The position of one particle can be used to determine the positions of other particles.

We have also studied the real-time dynamics of the system under sudden quenches. Two perturbations have been explored: a change in the trapping frequency and a change in the interaction strength. The former excites both CM and relative modes, while the latter excites only relative modes. These dynamical probes have allowed us to extract excitation gaps and gain insight into the spectral structure of the system. However, limitations in numerical resolution—especially for higher excited states—have restricted our ability to fully reconstruct the spectrum.

Overall, this work offers a detailed picture of the equilibrium and nonequilibrium behavior of p-wave fermions across the full interaction landscape. In particular, the regime $g_{\mathrm{F}} \to 0^+$ emerges as an especially rich and subtle limit, warranting further investigation. Improved numerical resolution in position space is essential to accurately capture the divergent correlations in this regime. The behavior of the eigenvalues of the OBDM in this limit may serve as a sensitive probe for distinguishing fermionic from bosonic character. Finally, the square well representation introduced here could serve as a useful numerical tool for future studies. From an experimental perspective, tracking the evolution of the system after parameter quenches may offer a practical route to access its excitation spectrum.

Bibliography

[1] I. Bloch, J. Dalibard, S. Nascimbène. Quantum simulations with ultracold quantum gases. *Nature Physics*, 8(4):267–276, 2012.

[2] M. Lewenstein, A. Sanpera, V. Ahufinger, B. Damski, A. Sen(De), U. Sen. Ultracold atomic gases in optical lattices: mimicking condensed matter physics and beyond. *Advances in Physics*, 56(2):243–379, 2007.

[3] N. Goldman, J. C. Budich, P. Zoller. Topological quantum matter with ultracold gases in optical lattices. *Nature Physics*, 12(7):639–645, 2016.

[4] I. Bloch. Ultracold quantum gases in optical lattices. *Nature Physics*, 1(1):23–30, 2005.

[5] W. D. Phillips. Nobel lecture: Laser cooling and trapping of neutral atoms. *Rev. Mod. Phys.*, 70:721–741, 1998.

[6] H. J. Metcalf, P. Van der Straten. *Laser cooling and trapping*. Springer Science & Business Media, 1999.

[7] K. Bongs, S. Burger, S. Dettmer, D. Hellweg, J. Arlt, W. Ertmer, K. Sengstock. Waveguide for bose-einstein condensates. *Phys. Rev. A*, 63:031602, 2001.

[8] T. L. Gustavson, J. R. Abo-Shaeer, A. P. Chikkatur, S. Gupta, S. Inouye, T. Rosenband, W. Ketterle A. Görlitz, J. M. Vogels, A. E. Leanhardt, C. Raman. Realization of bose-einstein condensates in lower dimensions. *Phys. Rev. Lett.*, 87:130402, 2001.

[9] H. Moritz, T. Stöferle, M. Köhl, T. Esslinger. Exciting collective oscillations in a trapped 1d gas. *Phys. Rev. Lett.*, 91:250402, 2003.

[10] K. Kanjilal, D. Blume. Nondivergent pseudopotential treatment of spin-polarized fermions under one- and three-dimensional harmonic confinement. *Phys. Rev. A*, 70:042709, 2004.

[11] M. D. Girardeau, E. M. Wright. Static and dynamic properties of trapped fermionic tonks-girardeau gases. *Phys. Rev. Lett.*, 95:010406, 2005.

[12] M. Girardeau. Relationship between systems of impenetrable bosons and fermions in one dimension. *Journal of Mathematical Physics*, 1(6):516–523, 1960.

[13] L. Tonks. The complete equation of state of one, two and three-dimensional gases of hard elastic spheres. *Phys. Rev.*, 50:955–963, 1936.

[14] M. D. Girardeau, M. Olshanii. Fermi-bose mapping and n-particle ground state of spin-polarized fermions in tight atom waveguides, 2003.

[15] M. D. Girardeau, M. Olshanii. Theory of spinor fermi and bose gases in tight atom waveguides. *Phys. Rev. A*, 70:023608, 2004.

[16] H. Grosse, E. Langmann, C. Paufler. Exact solution of a 1d quantum many-body system with momentum-dependent interactions. *Journal of Physics A: Mathematical and General*, 37(16):4579–4592, 2004.

[17] J. R. Taylor. *Scattering Theory: The Quantum Theory of Nonrelativistic Collisions*. John Wiley & Sons, New York, 2nd edition, 1972.

[18] M.D. Girardeau, H. Nguyen, M. Olshanii. Effective interactions, fermi–bose duality, and ground states of ultracold atomic vapors in tight de broglie waveguides. *Optics Communications*, 243(1):3–22, 2004.

[19] F. Sabater, A. Rojo-Francàs, G. E. Astrakharchik, B. Juliá-Díaz. A bcs state formulation for the fermionic tonks-girardeau gas, 2024.

[20] T. Cheon, T. Shigehara. Fermion-boson duality of one-dimensional quantum particles with generalized contact interactions. *Phys. Rev. Lett.*, 82:2536–2539, 1999.

[21] T. Busch, B.-G. Englert, K. Rzażewski, M. Wilkens. Two cold atoms in a harmonic trap. *Foundations of Physics*, 28(4):549–559, 1998.

[22] J. B. McGuire. Study of exactly soluble one-dimensional n-body problems. *Journal of Mathematical Physics*, 5(5):622–636, 1964.

[23] P. Kościk, T Sowiński. Variational ansatz for p-wave fermions confined in a one-dimensional harmonic trap. *New Journal of Physics*, 22(9):093053, 2020.

[24] F. Sabater, A. Rojo-Francàs, G. E. Astrakharchik, B. Juliá-Díaz. Universal composite boson formation in strongly interacting one-dimensional fermionic systems. *Phys. Rev. Lett.*, 132:193401, 2024.

[25] S. Bauch, D. Hochstuhl, K. Balzer, M. Bonitz. Quantum breathing mode of interacting particles in harmonic traps. *Journal of Physics: Conference Series*, 220(1):012013, 2010.

[26] W. Tschischik, R. Moessner, M. Haque. Breathing mode in the bose-hubbard chain with a harmonic trapping potential. *Phys. Rev. A*, 88:063636, 2013.

[27] A. D. Kerin, A. M. Martin. Arbitrary interaction quench phenomena in harmonically trapped two-body systems. *Phys. Rev. A*, 109:033307, 2024.

[28] M. Moeckel, S. Kehrein. Interaction quench in the hubbard model. *Phys. Rev. Lett.*, 100:175702, 2008.

[29] P. Kościk. Optimized configuration interaction approach for trapped multiparticle systems interacting via contact forces. *Phys. Lett. A*, 382(36):2561–2564, 2018.

[30] A. Rojo-Francàs, A. Polls, B. Juliá-Díaz. Static and dynamic properties of a few spin 1/2 interacting fermions trapped in a harmonic potential. *Mathematics*, 8(7), 2020.

A Solving s-wave bosons with optimized exact diagonalization

We solve the problem of s-wave spin-aligned bosons in a one-dimensional ($1D$) harmonic trap using the optimized exact diagonalization (ED) method [29] in second quantization. The method involves performing ED on a basis that incorporates n_{OED} variational parameters. The energy spectrum is obtained by exploring the n_{OED} variational parameter space and performing ED at each point.

The Hamiltonian of the system is

$$\hat{\mathcal{H}}_{\mathrm{B}} = \sum_{i=1}^{N} \left(-\frac{\hbar^2}{2m}\partial_{x_i}^2 + \frac{1}{2}m\omega^2 x_i^2 + \sum_{j>i}^{N} g_{\mathrm{B}}\hat{\delta}_{ij} \right). \tag{36}$$

In the numerical simulation, we use the basis

$$\psi_n(x) = \frac{1}{\sqrt{2^n n!}} \left(\frac{m\Omega}{\pi\hbar}\right)^{1/4} \exp\left(-\frac{m\Omega x^2}{2\hbar}\right) H_n\left(\sqrt{\frac{m\Omega}{\hbar}}x\right), \tag{37}$$

where $n = 0, 1, 2, \ldots$, and $H_n(x)$ are the Hermite polynomials. The parameter Ω is the variational parameter used to minimize the ground state (GS) energy obtained from the ED. Since the basis is continuous, the s-wave interaction Eq. (11) can be rewritten simply as $\delta(x_i - x_j)$.

To facilitate numerical computations, the Hamiltonian is rewritten as:

$$\hat{\mathcal{H}}_{\mathrm{B}} = \sum_{i=1}^{N} \left(\underbrace{-\frac{\hbar^2}{2m}\partial_{x_i}^2 + \frac{1}{2}m\Omega^2 x_i^2}_{(n+1/2)\hbar\Omega} + \underbrace{\frac{1}{2}m(\omega^2 - \Omega^2)x_i^2}_{\hat{V}_{\mathrm{extra}}} + \sum_{j>i}^{N} g_{\mathrm{B}}\hat{\delta}_{ij} \right). \tag{38}$$

The extra potential, $\hat{V}_{\mathrm{extra}}$, in second quantization becomes:

$$\hat{V}_{\mathrm{extra}} = \sum_{ij} \frac{1}{2}m(\omega^2 - \Omega^2) \langle i| x^2 |j\rangle \hat{a}_i^\dagger \hat{a}_j. \tag{39}$$

The matrix elements $\langle i| x^2 |j\rangle$ are expressed as

$$\begin{aligned} \langle i| x^2 |j\rangle &= \frac{1}{\sqrt{2^{i+j} i! j!}} \left(\frac{m\Omega}{\pi\hbar}\right)^{1/2} \int e^{-m\Omega x^2/\hbar} x^2 H_i\left(\sqrt{\frac{m\Omega}{\hbar}}x\right) H_j\left(\sqrt{\frac{m\Omega}{\hbar}}x\right) dx \\ &= \frac{1}{\sqrt{2^{i+j} i! j! \pi}} \left(\frac{\hbar}{m\Omega}\right) \int e^{-\tilde{x}^2} \tilde{x}^2 H_i(\tilde{x}) H_j(\tilde{x}) \, d\tilde{x}, \end{aligned} \tag{40}$$

where $\tilde{x} \equiv x\sqrt{\frac{m\Omega}{\hbar}}$. The integral is analytically solvable:

$$\begin{aligned} I_{ij}^{\mathrm{extra}} &\equiv \frac{1}{\sqrt{2^{i+j} i! j! \pi}} \int e^{-\tilde{x}^2} \tilde{x}^2 H_i(\tilde{x}) H_j(\tilde{x}) \, d\tilde{x} \\ &= \frac{1}{2}\left(\sqrt{i(i-1)}\delta_{j,i-2} + (2i+1)\delta_{j,i} + \sqrt{(i+2)(i+1)}\delta_{j,i+2} \right). \end{aligned} \tag{41}$$

The s-wave interaction term in second quantization is

$$\frac{g_{\mathrm{B}}}{2} \sum_{i,j,k,l} (ij|\delta(x_1 - x_2)|kl) \hat{a}_i^\dagger \hat{a}_j^\dagger \hat{a}_l \hat{a}_k = \frac{g_{\mathrm{B}}}{2}\sqrt{\frac{m\Omega}{\hbar}} \sum_{i,j,k,l} I_{ijkl} \hat{a}_i^\dagger \hat{a}_j^\dagger \hat{a}_l \hat{a}_k, \tag{42}$$

where $I_{ijkl} \equiv (ij|\delta(\tilde{x}_1 - \tilde{x}_2)|kl)$, and it has an analytical solution [30]

$$\begin{aligned} I_{ijkl} =& \frac{1}{\pi^2\sqrt{2}} \sum_{r=0}^{l} \sqrt{\frac{k!l!}{i!j!}} \frac{1}{r!(l-r)!(k-l+r)!} \Gamma\left(\frac{i+j-k+l-2r+1}{2}\right) \\ & \times \Gamma\left(\frac{i-j+k-l+2r+1}{2}\right) \Gamma\left(\frac{-i+j+k-l+2r+1}{2}\right), \end{aligned} \tag{43}$$

where we assume $l \leq k$. The complete Hamiltonian in second quantization becomes

$$\begin{aligned} \hat{\mathcal{H}}_{\mathrm{B}} =& \sum_i \left(\hat{a}_i^\dagger \hat{a}_i + \frac{1}{2}\right) \hbar\Omega + \sum_{i,j} \frac{1}{2} m(\omega^2 - \Omega^2) \left(\frac{\hbar}{m\Omega}\right) I_{ij}^{\mathrm{extra}} \hat{a}_i^\dagger \hat{a}_j + \\ & + \frac{g_{\mathrm{B}}}{2} \sqrt{\frac{m\Omega}{\hbar}} \sum_{i,j,k,l} I_{ijkl} \hat{a}_i^\dagger \hat{a}_j^\dagger \hat{a}_l \hat{a}_k. \end{aligned} \tag{44}$$

This form of the Hamiltonian allows for more efficient computation. In the context of ED, the matrix elements do not need to be recomputed for every value of Ω.

B The s-wave interaction as a square well

Consider two spin-aligned s-wave bosons in free space. The Hamiltonian of this system is

$$\hat{\mathcal{H}}_{\mathrm{B}} = -\frac{\hbar^2}{2m}\partial_{x_1}^2 - \frac{\hbar^2}{2m}\partial_{x_2}^2 + g_{\mathrm{B}}\hat{\delta}_{12}. \tag{45}$$

This Hamiltonian is separable in the coordinates of the center of mass (CM), X, and the relative position between the two particles, x. The solutions to the CM Hamiltonian are plane waves. For $g_{\mathrm{B}} < 0$, the relative part exhibits a bound state, and its wave function is given by [22]:

$$\psi_{\mathrm{rel}}(x) = \sqrt{\frac{g_{\mathrm{B}}\mu}{2\hbar^2}} e^{|x|g_{\mathrm{B}}\mu/\hbar^2}, \tag{46}$$

with energy $E_{\mathrm{rel}} = -\mu g_{\mathrm{B}}^2/(2\hbar^2)$. To solve the problem numerically in position space, the space is discretized. The structure of the mesh determines the form of the potential. We use the mesh: $\{-L, -L+\Delta x, \ldots, -\Delta x, 0, \Delta x, \ldots, L-\Delta x, L\}$. It can be shown that, on this mesh, the square well is nonzero at $x = 0$ with height

$$V_{x=0} = \frac{\hbar^2}{2\mu} \frac{\psi_{\mathrm{rel}}(\Delta x) - 2\psi_{\mathrm{rel}}(0) + \psi_{\mathrm{rel}}(-\Delta x)}{\Delta x^2 \psi_{\mathrm{rel}}(0)} + E_{\mathrm{rel}} = \frac{\hbar^2}{\mu} \frac{e^{g_{\mathrm{B}}\Delta x\mu/\hbar^2} - 1}{\Delta x^2} - \frac{\mu g_{\mathrm{B}}^2}{2\hbar^2} \approx \frac{g_{\mathrm{B}}}{\Delta x}, \tag{47}$$

where we use the Taylor expansion $e^x \sim 1 + x$. Therefore, the discrete representation of the interaction $g_{\mathrm{B}}\hat{\delta}_x$ is a square well of height $g_{\mathrm{B}}/\Delta x$ located at $x = 0$, and zero elsewhere. This suggests that, in general, the Dirac delta is represented in discrete space by $1/\Delta x$ at a single mesh point. This well-known representation is commonly used in numerical simulations. Nevertheless, this derivation provides a potential methodology for deriving a general expression for the p-wave interaction.

C Pair correlation matrix for $N = 2$

For $g_{\mathrm{F}} \to -\infty$, the pair correlation matrix corresponds to that of N ideal bosons in the GS, with zero on the diagonal. As the interaction strength increases from negative infinity to zero, the fermions gradually separate, reaching the non-interacting limit at $g_{\mathrm{F}} \to 0^-$. In $g_{\mathrm{F}} \to 0^+$, the fermions are next to each other. As the interaction strength increases, they begin to separate, and the pair correlation matrix once again converges to the FTG limit in the infinitely interacting limit, $g_{\mathrm{F}} \to +\infty$.

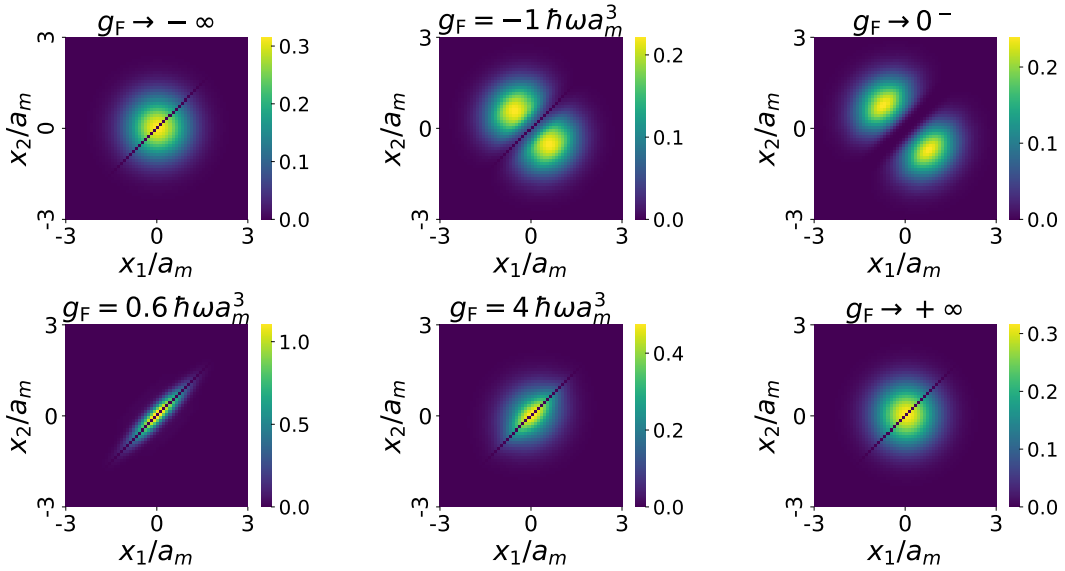

Figure 12: Pair correlation matrix of the GS for two p-wave fermions in a harmonic trap at six different interaction strengths. The limits $g_F \to \pm\infty$ correspond to the FTG limit, while $g_F \to 0^-$ corresponds to the non-interacting limit. The case of $g_F = 0.6\,\hbar\omega a_m^3$ represents a regime of strong correlations. The remaining two values correspond to intermediate interaction strengths, illustrating the transition between the limiting cases.